1998

Effects of Frost Formation on the External Heat Transfer Coefficient of a Counter-Crossflow Display Case Air Coil

W. T. Horton
Purdue University

E. Groll
Purdue University

Effects of Frost Formation on the External Heat Transfer Coefficient of a Counter-Crossflow Display Case Air Coil

W. Travis Horton[1] and Eckhard Groll[2]

Ray W. Herrick Laboratories
Purdue University
West Lafayette, IN 47907-1077, USA

Abstract

Frost formation on the cooling coils of supermarket display cases causes a reduction in the operating efficiency of the refrigeration equipment. In order to optimize the defrost cycle of such systems it is important to study and understand the effects of frost formation. This paper presents the air side heat transfer coefficient results for an air coil that is typically used in supermarket applications.

Nomenclature

A_{coil} = exterior surface area of the coil [m^2]
A_i = internal tube area [m^2]
D = tube diameter [m]
Δh = change in specific enthalpy [kJ/kg]
ΔT_{lm} = log mean temperature difference [K]
h_i = inside heat transfer coefficient [W/(m^2 K)]
h_o = outside heat transfer coefficient [W/(m^2 K)]
h_{eff} = effective outside heat transfer coeff.
k = thermal conductivity [W/(m K)]
Nu_D = Nusselt number (h D/k)
Pr = Prandtl number
Q = heat transfer rate [W]
R_w = thermal impedance of tube wall [K/W]
U = overall heat transfer coeff. [W/(m^2 K)]

Introduction

Increasing interest with respect to the efficiency of modern HVAC&R equipment has led researchers to study and optimize the different components of HVAC&R systems. Some of the components that are constantly being studied and improved are the heat exchangers in a vapor compression cycle. Frost formation on the evaporator of a direct expansion vapor compression cycle causes a reduction in heat transfer capacity and reduces the overall cycle efficiency. Further frost formation will cause the cooling capacity to continue to decrease until the system must be turned off and the evaporator defrosted. Supermarkets face many cost related issues due to frost formation and the subsequent defrosting of display case air coils. When the vapor compression cycle is turned off and the defrost cycle is activated to melt the ice on the air coil, there is an increase in temperature of the food products that are in the display case. Depending on the length of the defrost cycle the food temperature increase may exceed the maximum

---
[1] Graduate Research Assistant, Purdue University
[2] Assistant Professor of Mechanical Engineering, Purdue University

allowable temperature. In humid climates, infrequent defrosting may result in high product temperatures, while frequent defrosting in dryer climates may result in excessive energy consumption. In order to optimize the frequency and duration of the defrost cycle it is important to study the formation of frost and its associated effects on the overall heat transfer coefficient of a heat exchanger that is typically used in supermarket applications.

Test Setup

Testing was conducted in a closed loop psychrometric wind tunnel, shown schematically in Figure 1. A variable speed controller allowed coil face velocities to vary from 100 to 400 ft/min. A preconditioning (dehumidification) coil was located directly downstream of the blower, followed by steam injection, electric reheat, and a flow mixer. This facility provides complete control over the temperature, humidity, and air flow rate at the inlet to the test section. Downstream of the test coil, a nozzle constructed to ASHRAE standards was located which allows measurement of the volumetric airflow rate. The test facility is fully instrumented to measure the pressure drop across the test section as well as the dry bulb temperature and relative humidity before and after the test section.

The test unit consisted of an air coil, located in the wind tunnel, that is typically used in supermarket display cases. For the first set of tests the coil was connected to the compressor and condenser of an R-22 condensing unit while two other sets of tests were conducted using a chilled water glycol mixture as well as hydrofluoroether (HFE). The air coil has dimensions of 36 inch wide by 6 inch tall and 10 inch deep. The fin spacing was two fins per inch. A single circuit consisting of 32 copper tubes (5/8" OD) in a counter crossflow arrangement completed the coil. The compressor and condenser were located in a psychrometric chamber capable of simulating a constant outdoor temperature and humidity level of 70°F and 50% relative humidity.

Multiple tests were conducted with air face velocities of 100, 250, and 400 ft/min, with an air-side inlet temperature to the test section of 42°F (5.5°C) and 70% relative humidity. Furthermore, two additional tests were conducted at face velocities of 150 and 300 ft/min. During the direct expansion R-22 tests, the evaporation temperature was held constant at 16°F (-9°C). During the secondary fluids tests, the inlet temperature of the secondary fluid was held constant at 25°F (-4°C). The test procedure began by starting the wind tunnel and allowing the air to achieve steady state inlet conditions at 42°F (5.5°C) and 70% relative humidity. When the inlet conditions had stabilized, the direct expansion test unit was started and the superheat adjusted to approximately 20°F (10°C). Following superheat stabilization the test unit was allowed to run for a period of 1.5 to 2 hours.

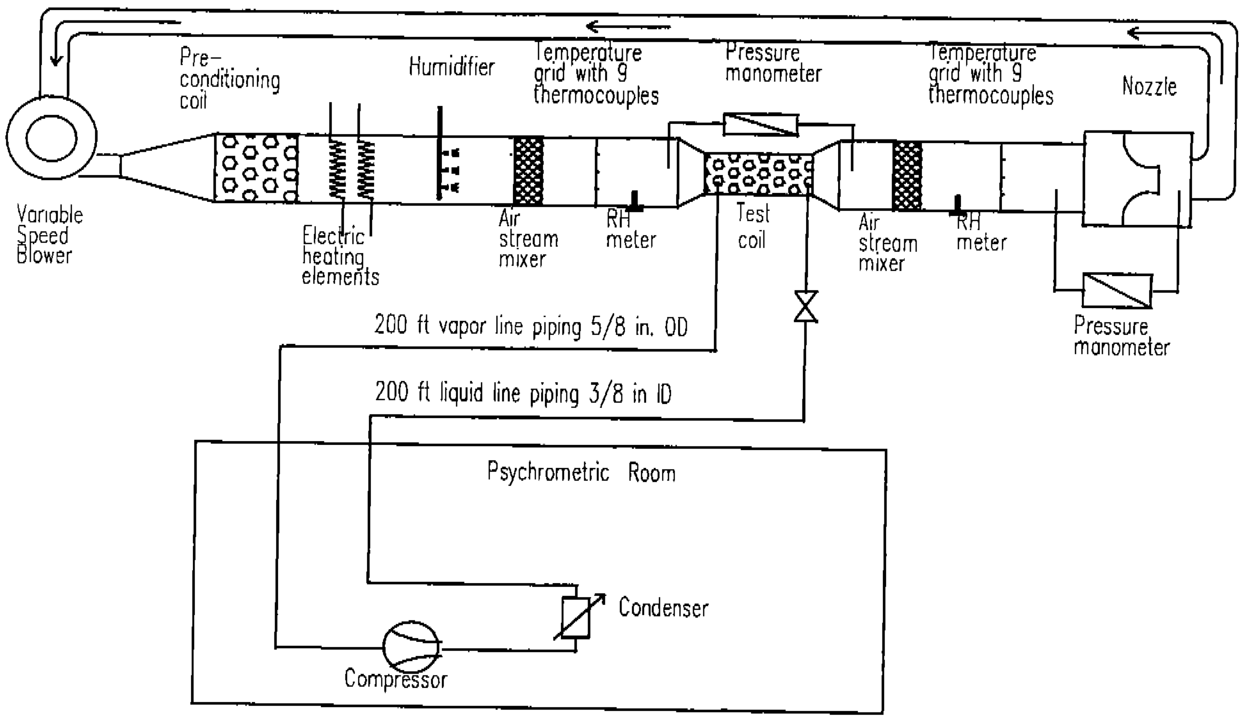

Figure 1: Wind Tunnel Test Facility

Analysis

To determine the overall heat transfer coefficient, the following equation (Incropera and DeWitt, 1992), based on the external surface area of the air coil, may be employed

$$\dot{Q} = UA_{coil}\Delta T_{lm} \tag{1}$$

Once the total heat transfer rate, the heat exchanger surface area, and log mean temperature difference are known, the equation can be solved for the overall heat transfer coefficient. The air coil heat transfer rate may be determined by applying the following first law equation to the refrigerant

$$\dot{Q} = \dot{m}_{ref}\Delta h \tag{2}$$

Additionally, the log mean temperature difference may be defined as

$$\Delta T_{lm} = \frac{\Delta T_2 - \Delta T_1}{\ln\left(\Delta T_2 / \Delta T_1\right)} \tag{3}$$

where ΔT_1 and ΔT_2 are given by the expressions

$$\Delta T_1 = T_{air,in} - T_{ref,out}$$
$$\Delta T_2 = T_{air,out} - T_{ref,in} \quad (4)$$

The air coil under consideration has an external surface area of 6.4 m^2. Once the overall heat transfer coefficient has been determined it is then possible to calculate the external convective heat transfer coefficient according to the equation

$$\frac{1}{UA_{coil}} = \frac{1}{\eta h_o A_{coil}} + R_w + \frac{1}{h_i A_i} \quad (5)$$

where the first term on the right hand side represents the external resistance to convective heat transfer from the surface of the heat exchanger to the airstream, while the second term represents the conductive thermal impedance through the walls of the tube and the third is the internal resistance to convective heat transfer.

Results

Figure 2 shows the results of the overall heat transfer coefficient as a function of the face velocity for the three sets of test data using water glycol, HFE, and R22 as the working fluids. As would be expected, the overall heat transfer coefficient increases as a function of increasing face velocity.

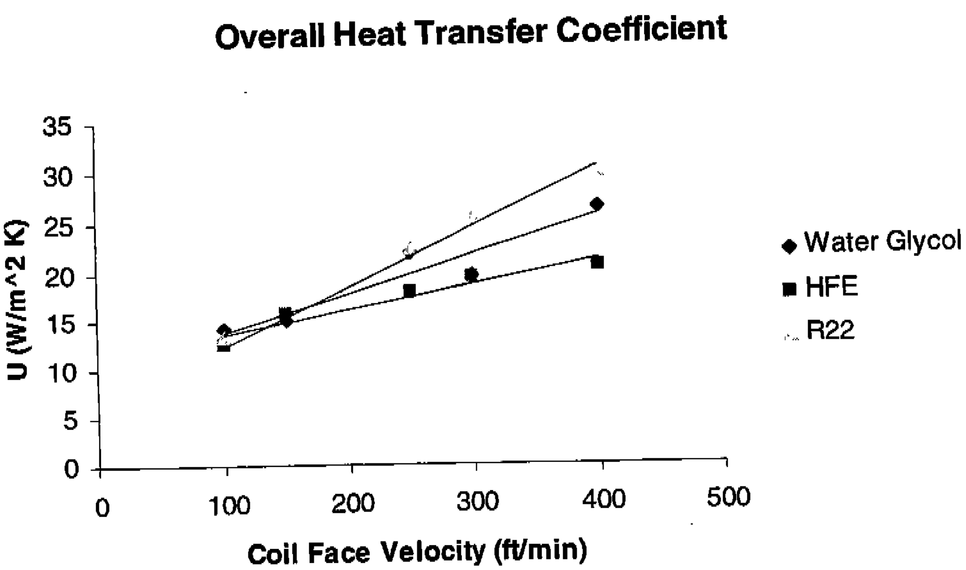

Figure 2: Overall heat transfer coefficient versus face velocity

Given the overall heat transfer coefficient, the next step was to calculate the external convective heat transfer coefficient according to equation (5). The internal convective heat transfer coefficient can be determined by the Dittus-Boelter correlation (Dittus and Boelter, 1930)

$$Nu_D = 0.023\,Re_D^{\frac{4}{5}}\,Pr^{0.4} \tag{6}$$

Since it is impossible in the current test setup to distinguish between the change in the wall thermal resistance as frost forms and the change in the outside convective heat transfer coefficient, the first two terms on the right hand side of equation (5) can be lumped together into an effective outside heat transfer coefficient and equation (5) can be rewritten as

$$\frac{1}{UA_{coil}} = \frac{1}{h_{eff}A_{coil}} + \frac{1}{h_i A_i} \tag{7}$$

Equations (6) and (7) can be solved to determine the effective outside heat transfer coefficient for the two test sets using water glycol and HFE. The results of these calculations are given in Figure 3, which may be used to establish the effective outside heat transfer coefficient for the case when no frost is present on the air coil. Knowing the effective outside heat transfer coefficient for the case of no frost formation gives a starting point for the R-22 tests where there was substantial frost formation. Figure 4 shows the effective heat transfer coefficient over time for R-22 tests with face velocities of 100, 250, and 400 ft/min. Figure 4 shows that the formation of frost reduces the effective outside heat transfer coefficient over time almost linearly.

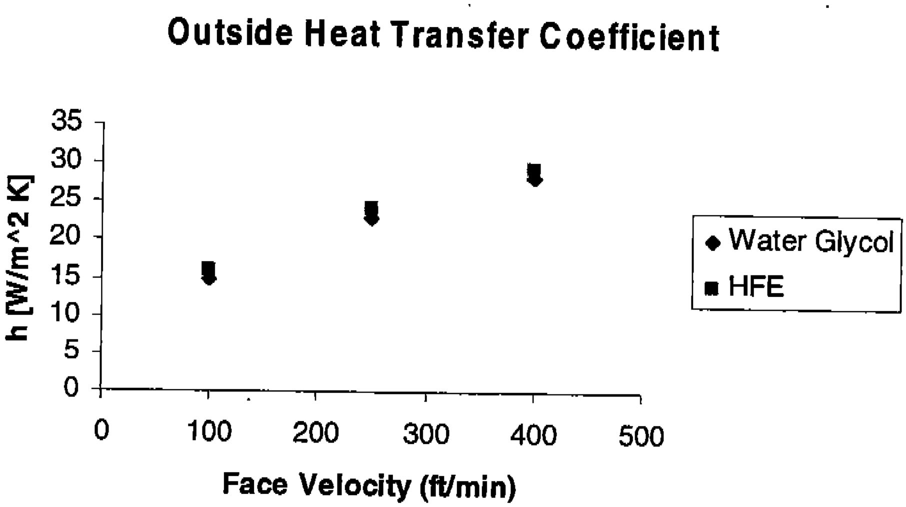

Figure 3: Effective outside heat transfer coefficient when no frost is present versus face velocity

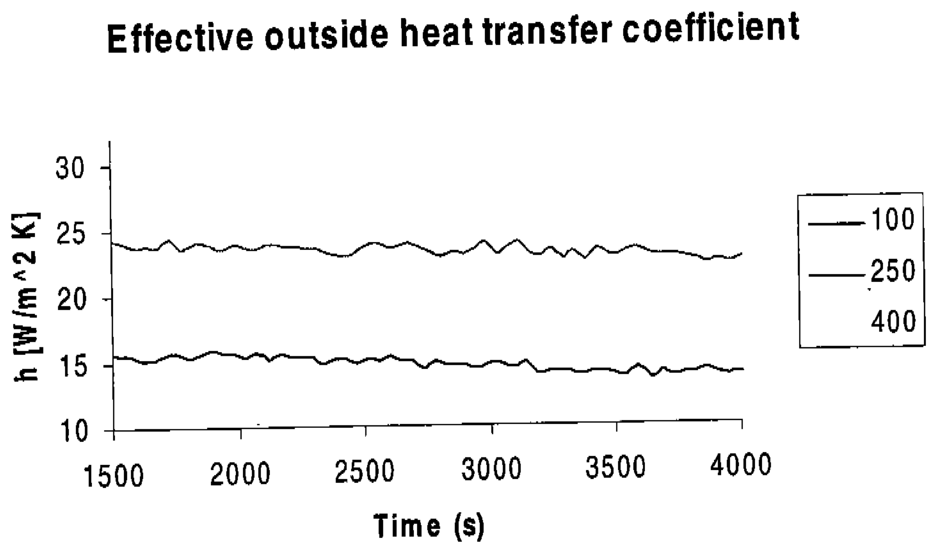

Figure 4: Effective outside heat transfer coefficient during frost formation over time

Conclusions

The data that has been collected in this study will provide vital information in the verification of a dynamic simulation model for display case air coils, which is currently under development by the authors. As increasing importance is placed on the efficient operation of refrigeration equipment, such as supermarket refrigeration systems, it is critical to study the effects of frost formation on the performance of cooling coils.

References

Incropera, F.P, & DeWitt, D.P. "Fundamentals of Heat and Mass Transfer," John Wiley & Sons, New York, 3rd ed., pp. 648-649, 1990.

Dittus, F.W., & Boelter, L.M.K., University of California Publications on Engineering, Vol. 2, pp. 443, Berkeley, 1930.